BEYOND FINGERPRINTS MORPHOLOGY: CHEMICAL MAPPING OF FUNCTIONAL GROUPS

F. Cervelli[1,*], *S. Carrato*[2], *A. Mattei*[1], *L. Benevoli*[3], *L. Vaccari*[3]

[1] Raggruppamento Carabinieri Investigazioni Scientifiche, Italy
[2] Dipartimento di Ingegneria Industriale e dell'Informazione, Trieste, Italy
[3] Sincrotrone Trieste, Trieste, Italy

ABSTRACT

Fingerprints are one the oldest biometrics used in investigations. The fingerprint morphology is considered unique and immutable and it is routinely used to identify an individual from the mark found at the crime scene. The comparison is based solely on the ridges flow and on their discontinuities (i.e. the minutiae), without considering other information possibly embedded in the fingerprint itself. In this work we used a Fourier Transform Infrared microspectroscopy (FT-IRMS) to obtain the morphology and the chemical map of functional groups in fingerprints. The FT-IRMS technique is able to acquire hyperspectral images of the organic compounds present in the samples under examination. However both sophisticated processing and user interaction are required to process the spectra, and no fully automated procedure is currently available.

We prepared a set of test fingerprints and collected the data with the FT-IRMS; we then developed an automated procedure to process the data without user interaction and were able to produce maps related to fingerprint deposits. More in details, the developed system is able to produce both integral maps, providing a summary of the contribution in a specific wavelength range, and peak maps, which show the contribution of a selected functional group. The automatic processing steps, although born with the fingerprint in mind, are fairly general, and can be applied to all fields where there is the need to process a large amount of spectra without user interaction.

Index Terms— Fingerprints, Functional groups, Chemical mapping, Automated analysis, Spectra

1. INTRODUCTION

Fingerprints are one the oldest biometrics used in investigations. The fingerprint morphology is considered unique and immutable and it is routinely used to identify an individual from the finger mark found at the crime scene. The comparison is based solely on the flow of the ridges and on their discontinuities, the so called *minutiae*: the higher the number of corresponding minutiae the higher the probability of the match.

Fingerprint evidence has been already proven to be more than useful for identification; however, only the morphology has been used so far, and no other information has been looked for. As a matter of fact, during the crime all involved individuals interact both with each other and with the crime scene environment; thus they come in contact with different materials related to the crime [1], and a fingerprint found on the crime scene may have recorded this additional information. Being able to relate a fingerprint to the crime, e.g. finding blood, semen, glass fragments or lipstick residues in it, would be valuable for the investigation both to understand the crime dynamics and to prosecute the culprit.

FT-IRMS has been already used to analyze particles and droplets that constitute fingerprint ridge deposits [2]: sample fingerprints were deposited on purpose on aluminum coated slides before and after washing the hands to produce eccrine and sebaceous fingerprints. Eccrine fingerprints were produced simply touching the surface with fingers after washing the hands; sebaceous fingerprints were produced washing the hands and then rubbing the forehead prior to touching the surface. Then a functional group analysis was performed on selected particles found in the different kind of fingerprints, showing the presence of esters of dicarboxylic acids and protein-containing skin cells.

In [3] four different substances (Ibuprofen, Vitamin C, Non-Dairy Creamer, and Sweet'N Low) were handled by the donors before depositing the test fingerprints on a gold plated glass. A microscope was then used to find the fingerprint particles, which were analyzed with infrared microspectroscopy to recognize the handled materials using a library built on purpose.

More recently a study looked for exogenous substances in fingerprints using a FTIR-Visible microscope [4]. Hands were washed and the index finger was rubbed on the face, neck and hair to produce sebaceous rich fingerprints. The finger was then lightly pressed into the powdered substance of interest and pressed onto either a metal oxide-coated glass slide or onto a silicon window. Substances of different nature were employed, ranging from pharmaceuticals (caffeine,

*Corresponding author: federico.cervelli@gmail.com.

aspirin, diazepam) to drug (cocaine), and explosive (PETN); finally the authors tested different spectral comparison algorithms to find the best one for accomplishing the task and demonstrated the usefulness of the system in case the fingerprints were deposited by the suspect after the crime.

In this work we used FT-IRMS to obtain not only the morphology but also the spatial distribution of molecular functional groups in fingerprints. Differently from other groups we evaluated the full fingerprint and developed a fully automated procedure for morphology and functional group analysis, overcoming a common problem of FT-IRMS analysis, i.e. the difficulty in the identification and quantification of close and partially overlapping peaks.

In Sec. 2 we describe the experimental setup and sample preparation. In Sec. 3 we describe the spectra analysis system and in the following Sec. 4 we give the results of fingerprint mapping. Finally in Sec. 5 we draw our conclusions.

2. EXPERIMENTAL SETUP

Human fingerprints were deposited on lightly doped silicon wafers. The prints were left by two male and two female donors in depletion series, i.e. the same finger was pressed 7 times on the silicon in order to provide progressively poorer versions of the same finger. Differently form previous works [2, 3, 4] we allowed fingerprints to be deposited without prior washing; this allows to properly simulate the fingerprint which is found at the crime scene.

The FT-IRMS technique was used to produce the chemical imaging of the fingerprints deposited on the silicon substrates, in order to characterize the chemical nature of the deposits. FT-IRMS measurements have been carried out at the SISSI beamline of Elettra [5].

Infrared spectroscopy exploits the absorption of the light at specific frequencies, which are characteristic of a given chemical bond. Because of this, the technique can detect, distinguish and determine the relative amount of both endogenous and exogenous chemicals constituting the fingerprint.

FT-IRMS exploits an interferometer (Fig. 1A). A polychromatic source of light S emits IR radiation which is sent to a beam splitter B, that partially transmits and partially reflects the incoming beam. The splitted beams travel to two mirrors, M1 (fixed) and M2 (movable), which reflect them back to B. The beams are superimposed at the beamsplitter and their interfernce pattern is recorder at the detector. The ratio between the Fourier transformed sample signal and the detected signal in air is the IR spectrum of the sample. In FT-IRMS, IR-Visible microscopes mounting optics able to focus both IR and visible light are coupled with the interferometric system, allowing to collect spatially resolved chemical information on the sample.

FT-IRMS spectra have been collected in the Mid-IR regime from 4000 to 900 cm^{-1} using a Bruker Vertex 70 interferometer equipped with a SiC glow bar source. The infrared beam was sent to a Hyperion 3000 Vis-IR microscope equipped with 15$\times$ cassegrain optics. FTIR spectra were collected in transmission mode by using a single-element Hg-Cd-Te detector. Using knife edge apertures and motorized stage we collected step-scan chemical maps of our samples by defining matrices of points of 100 $\times$ 100 μm^2. Data were acquired by averaging either 256 or 512 scans per point (the latter if the sample was particularly poor) at a frequency resolution of 16 cm^{-1}. Morphologically appropriate regions of fingerprints were then chemically characterized assembling maps of the collected spectra. Thus each picture element is not characterized by a single intensity value, but by a full spectrum, Fig. 1B.

Data collected by FT-IRMS must be processed to retrieve the desired chemical information [6, 7, 8]. This analysis can be performed following both multivariate and univariate approaches. The first are unsupervised approaches, such as Principal Component Analysis (PCA) or Hierarchical Cluster Analysis (HCA), that take into account the whole spectral information contained in the data (see [9] for a detailed overview of the multivariate approach). In the univariate approach, a specific infrared band, characteristic of the chemical compound of interest, is taken into account. Its spatial distribution is built either considering the signal intensity at a given wavelength or calculating the area under the specific spectral peak.

Since we know the rough wavelength position of the peaks of interest we chose the univariate analysis and functional group mapping, actually more representative of the chemistry of the sample.

In particular, we investigated the region between 1700 and 1500 cm^{-1}. As a matter of fact, characteristic bands of both fingerprint skin and sweat are in this range [2]. Proteins of skin cells exhibit two bands (the Amide I and the Amide II band) centered at about 1650 and 1550 cm^{-1}, respectively. The Amide I is mainly due to the carbonyl stretching of peptide bond, while the Amide II to the coupling of NH bending and CN stretching (Fig. 2A). Lactic acid of sweat can be identified by the carboxylic acid peak centred at around 1600 cm^{-1} (Fig. 2B). However, its overlapping with protein peaks can make difficult the proper location and quantification of both skin and sweat components.

3. FT-IRMS DATA PROCESSING

Spectral bands arising from the overlapping of different contributions need to be fitted in their components in order to retrieve information on each chemical compound contributing to the spectral shape.

The spectral preprocessing consists in the baseline correction. We estimated the baseline with the rubber band method [10] and then corrected all spectra by simple subtraction of the calculated baseline before proceeding with the fitting procedure.

Each baseline corrected spectra is modeled as a sum of Gaussian functions with different heights c_i, center frequen-

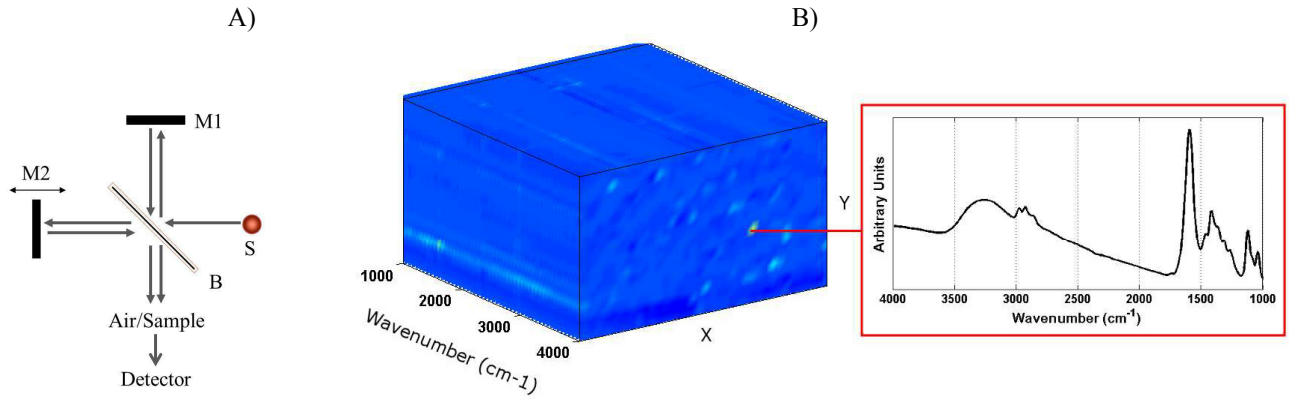

Fig. 1. A) Simplified optical scheme of an FTIR interferometer B) In FT-IRMS, a spectrum for each pixel of the sample is acquired.

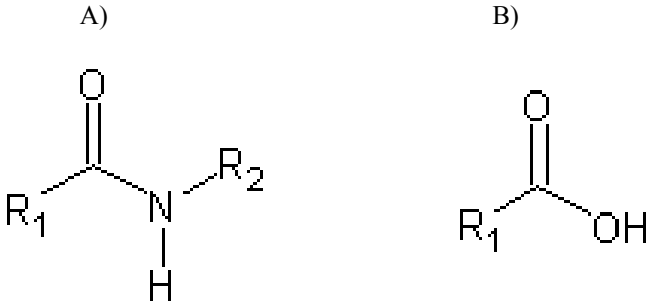

Fig. 2. Functional groups studied in this work: A) shows the Amide group, while B) shows the carboxylic.

cies k_i, and standard deviation σ_i. The number of Gaussians to be fitted is not fixed *a priori*: some spectra show only one Gaussian while others have more than six to consider. Thus we developed an automatic procedure to determine the number of Gaussian components to be used in the fit. Differently from the work presented in [11], the system is able to cope with structures hidden in the "shoulders" of spectra, thanks to the fact that it takes into account up to the third derivative of the spectra. Indeed, the candidate peaks in each spectrum are pointed out by the positive zero crossing of the third derivative, thus allowing the automatic estimation of the number of Gaussian curves to be used for the fit (Fig. 3).

Once the number of Gaussians has been fixed in the first step of the algorithm, the fitting procedure starts:

- in the first run the peak positions taken from the third derivative zero crossing are used as known parameters to evaluate the other fit parameters, i.e. the c_i and σ_i ;
- in the second run all parameters are initialized with the values calculated in the previous run and the Gaussians centers k_i are limited to vary in a fixed range ΔK (Fig. 4).

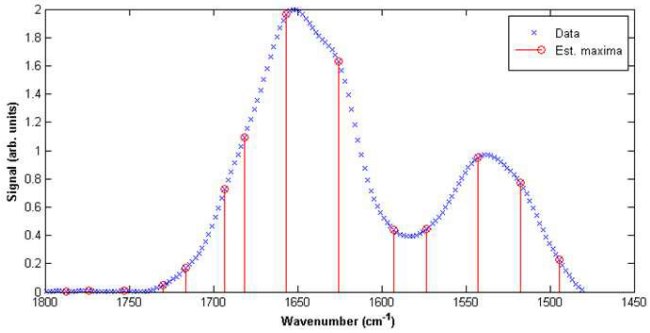

Fig. 3. During the first step of the algorithm the spectrum ($\times$) is processed in order to identify the number and positions of Gaussian maxima ($\circ$); these values are then considered fixed in this first run of the fitting procedure.

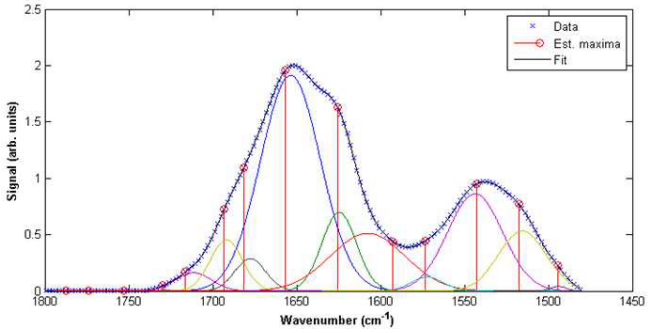

Fig. 4. During the second run of the fitting the spectrum ($\times$) is fitted considering all parameters as variable in a determined and chemically supported range; note that the positions of Gaussian maxima estimated in previous run ($\circ$) may be slightly different from the maxima found at the end of the procedure, as shown by the colored Gaussian components drawn below the spectrum.

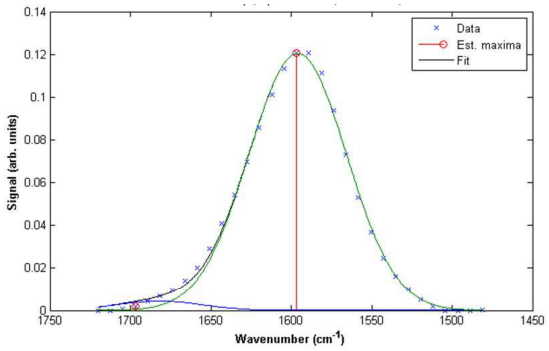

Fig. 5. Trying to estimate the contribution of functional groups around 1550 cm^{-1} would result in a fake signal, due to the important contribution of the group centered around 1500 cm^{-1}.

4. RESULTS

The results of the fitting procedure allow to obtain two different chemical maps:

- an *integral map* showing the total contribution of the chemical species in the selected frequency range of 1700–1500 cm^{-1};
- a *peak map* or *functional group map* for each functional group, useful to identify the contribution of each chemical specie.

With our procedure, once the Gaussians center frequencies k_i, standard deviations σ_i and heights c_i have been found, the contribution to each single spectrum of the Amide I and Amide II groups can be visualized by mapping only the parameters pertaining the Gaussians found nearby the Amide I or Amide II wavenumbers. This allows us to avoid a common problem in spectra analysis, i.e. the partial overlap of two (or more) close peaks which influence the computation of both their areas and their heights. An example is shown in Fig. 5: if we are interested in the contribution at 1550 cm^{-1}, the much stronger functional group around 1600 cm^{-1} would mask all other contributions to the spectrum.

The different maps obtained are shown in Fig. 6. Panel A shows the integral map obtained summing all contributions to the spectrum in the range 1565–1535 cm^{-1}. As it can be seen a high signal is present; however this is the pixel where the spectrum of Fig. 5 is located. Panel B shows the map built considering the functional group, i.e. built with the value of the height of the Gaussian centered at 1550 cm^{-1} as a result of the automatic fitting procedure; the fake strong signal of panel A is no more present in panel B, which correctly shows the contributions due only to the Gaussian component around 1550 cm^{-1}.

Thus, thanks to the proposed method, the acquired sample fingerprints were characterized via both their morphology and their content, either as an integral information or as a functional group representation, as shown in Fig. 7. Panel

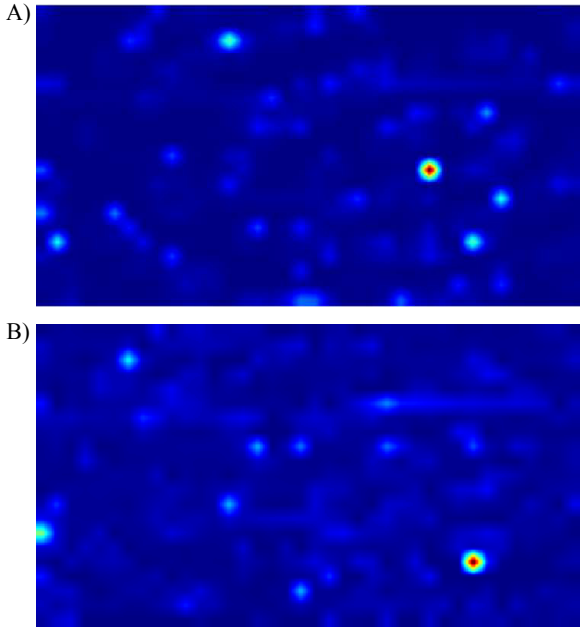

Fig. 6. The integral map obtained summing all contributions to the spectrum in the range 1565–1535 cm^{-1} is shown in A), while the functional group map representing the group centered at 1550 cm^{-1} is shown in B) as a result of the automatic fitting procedure; note that the fake strong signal in A is no more present in B.

A shows the fingerprint under study and panel B shows the matching morphology obtained by integrating the spectra in the 1700–1500 cm^{-1} range. Panels C and D show the contribution of the Amide I and of the carboxylic band, respectively.

5. CONCLUSIONS

Fingerprint coming from the real crime scenario are chemically quite complex, containing information on both endogenous and exogenous constituents. IR bands characteristic of each fingerprint constituent overlap together and the possibility to recognize, quantify and assign each of them is often the only solution to better understand the crime dynamics and to prosecute the culprit. IR band deconvolution gives this opportunity but this approach has been limited up to now by the lack of automated programs that can quickly process many spectra simultaneously, as needed when analyzing large IR images.

This is the obstacle we aimed at overcoming by proposing our automated procedure which deconvolves the IR bands by band fitting and is able to run over thousands of spectra without the bias of the operator. The choice of the silicon substrate has been done in order to have a good quality data set for testing the new algorithm, even if, of course, it is not representative of the real crime scenario. Reflection geometry, as well as Attenuated Total Reflection (ATR) sampling techniques can be used for real samples, such as fingerprint

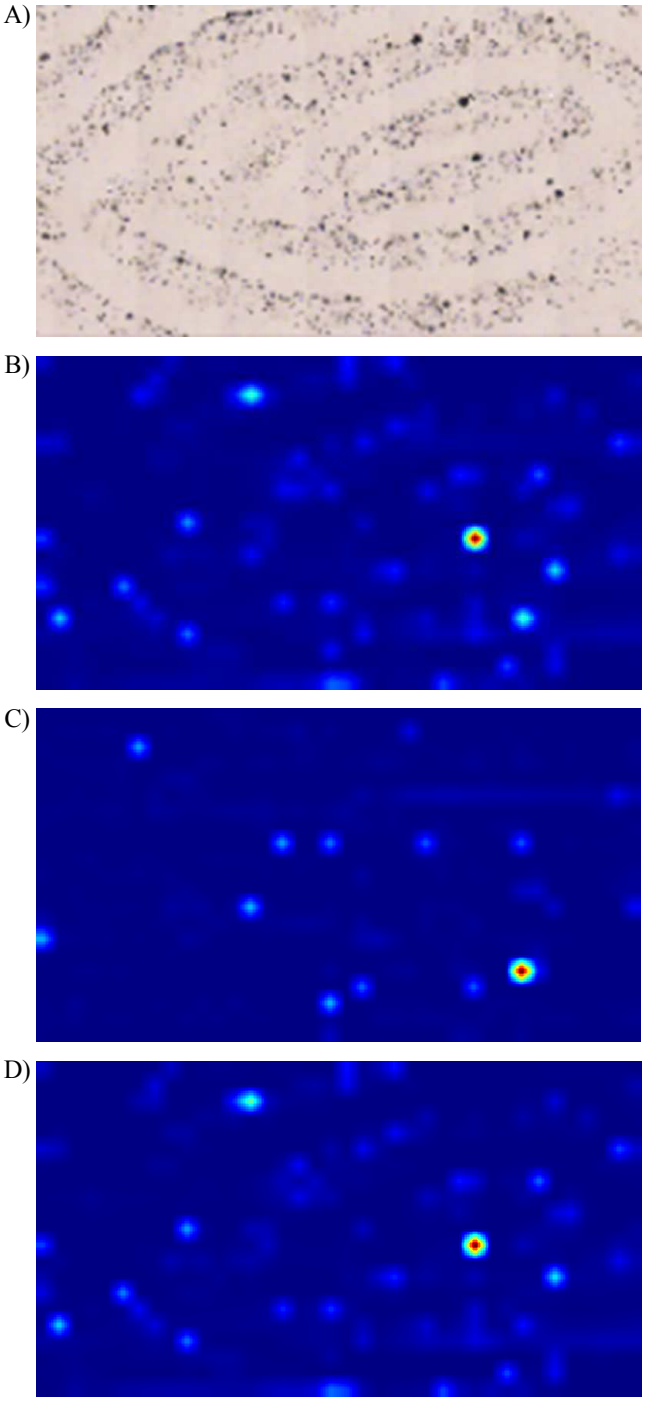

Fig. 7. A fingerprint can be characterized with its morphology and chemical content: A) fingerprint under study, B) integral map in the range 1700–1500 cm^{-1}, C) functional group map at 1650 cm^{-1}, D) functional group map at 1600 cm^{-1}. For the functional group map at 1550 cm^{-1} see Fig. 6B.

deposits on glass, plastic materials etc., without affecting the reliability of the fitting approach we propose.

Future works will be devoted to addressing the identification of forensically relevant compounds of the fingerprint, such as blood, semen and saliva, in order to provide more useful answers to the investigators.

6. REFERENCES

[1] J. Horswell and C. Fowler, *The Practice of Crime Scene Investigation*, chapter 2, CRC Press, London, 2004.

[2] D. K. Williams, R. L. Schwartz, and E. G. Bartick, "Analysis of latent fingerprint deposits by infrared microspectroscopy," *Applied Spectroscopy*, vol. 58, pp. 313–316, 2004.

[3] A. Grant, T. J. Wilkinson, D. R. Holman, and M. C. Martin, "Identification of recently handled materials by analysis of latent human fingerprints using infrared spectromicroscopy," *Applied Spectroscopy*, vol. 59, pp. 1182–1187, 2005.

[4] P.H.R. Ng, S. Walker, M. Tahtouh, and B. Reedy, "Detection of illicit substances in fingerprints by infrared spectral imaging," *Anal. Bioanal. Chem.*, vol. 394, pp. 2039–2048, 2009.

[5] Elettra Synchrotron Light Laboratory of Trieste, "http://www.elettra.trieste.it," site.

[6] W. Herres and J. Gronholz, "Understanding FT-IR data processing. Part 1: data acquisition and Fourier transformation," *Comp. Appl. Lab.*, vol. 2, pp. 216–220, 1984.

[7] J. Gronholz and W. Herres, "Understanding FT-IR data processing. Part 2: details of the spectrum calculation," *Instruments and Computers*, vol. 3, pp. 10–16, 1985.

[8] J. Gronholz and W. Herres, "Understanding FT-IR data processing. Part 3: further useful computational methods," *Intell. Instrum. Comp.*, vol. 3, pp. 45–55, 1985.

[9] C. Gendrin, Y. Roggo, and C. Collet, "Pharmaceutical applications of vibrational chemical imaging and chemometrics: a review," *J. Pharmaceutical Biomedical Analysis*, vol. 48, pp. 533–553, 2008.

[10] Bruker Optics, *Opus operating manual*, Bruker Optics, 2010.

[11] F. Cervelli, S. Carrato, A. Mattei, M. Jerian, L. Benevoli, L. Mancini, F. Zanini, L. Vaccari, A. Perucchi, and G. Aquilanti, "Imaging using synchrotron radiation for forensic science," in *Image Processing: Algorithms and Systems IX*, 2011, vol. 7870, pp. 78700B–1.